Inorganic Chemistry
Article
pubs.acs.org/IC

Copper(II) Complexes of Cyclams Containing Nitrophenyl Substituents: Push-pull Behaviour and Scorpionate Coordination of the Nitro Group

Massimo Boiocchi,[†] Carlo Ciarrocchi,[†] Luigi Fabbrizzi,[*,†] Maurizio Licchelli,[†] Antonio Poggi,[†] Miguel Vázquez López[§]

[†] Centro Grandi Strumenti, Università di Pavia, via Bassi 21, 27100 Pavia, Italy

[‡] Dipartimento di Chimica, Università di Pavia, via Taramelli 12, 27100 Pavia, Italy

[§] Departamento de Química Orgánica, Universidade de Santiago de Compostela, 15782 Santiago de Compostela, Spain

ABSTRACT: The three nitrophenyl-cyclam derivatives: 1-(4-nitrophenyl)-1,4,8,11-tetraazacyclotetradecane (**4-NBC**), 1-(2-nitrophenyl)-1,4,8,11-tetraazacyclotetradecane (**2-NBC**), and 1-(2,4-dinitrophenyl)-1,4,8,11-tetraazacyclotetradecane (**2,4-NBC**) in an MeCN solution specifically incorporate the Cu^{II} ion according to an irreversible process signaled by disappearance of the yellow color for a concentratio $c < 10^{-4}$ M and by a yellow-to-red color change for $c \geq 10^{-3}$, and have to be considered effective dosimeters of copper(II) salts. When present in the *ortho*- position of the nitrophenyl substituent, the $-NO_2$ group coordinate the Cu^{II} according to a scorpionate mode, while the metallocyclam system exhibits a *trans-I* configuration. In an MeCN solution the red *trans-I*-[Cu^{II}(**2-NBC**)]$^{2+}$ and *trans-I*-[Cu^{II}(**2,4-NBC**)]$^{2+}$ scorpionate complexes slowly convert into the violet *trans-III* scorpionate complexes. Kinetic aspects of the *trans-I*-to-*trans-III* configurational rearrangement have been investigated in detail for the [Cu^{II}(**2,4-NBC**)]$^{2+}$ system. In particular, the conversion is spectacularly accelerated by catalytic amounts of Cl^-, NCO^- and F^-. While for Cl^- and NCO^- the effect can be associated to the capability of the anion to stabilize through coordination a possible dissociative intermediate, the amazingly powerful effect of F^- has to be related to the preliminary deprotonation of one N−H fragment of the macrocycle, driven by the formation of the HF_2^- ion. Most of the metal complex species studied in solution have been isolated in a crystalline form and their molecular structure has been elucidated through X-ray diffraction studies. This study documents the first examples of effective metal coordination by the nitro group.

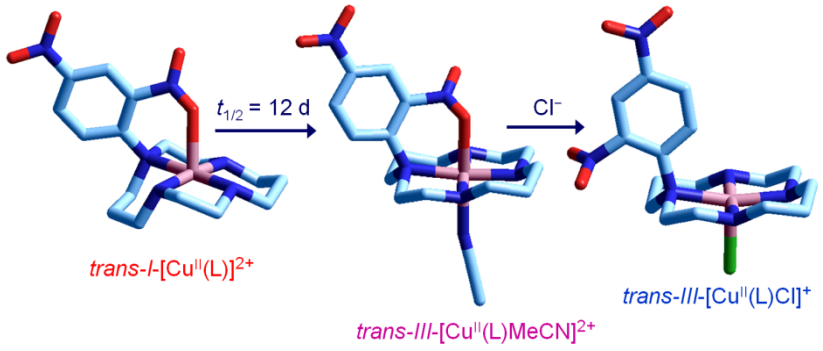

■ Introduction

N,N-dimethyl(4-nitro)-aniline (**1a**, DMNA) is a classical push-pull system D-Ph-A, in which a the dimethylamino *donor* group D and the nitro *acceptor* group A are connected via the π-conjugated system of a phenyl ring (Ph). The molecule exhibits a pronounced polar character, with $\mu_0 = 5.92$ D. On light absorption, the system is excited to the state **1b**, which involves a substantial transfer of electron density from D to A, as depicted in Scheme 1.

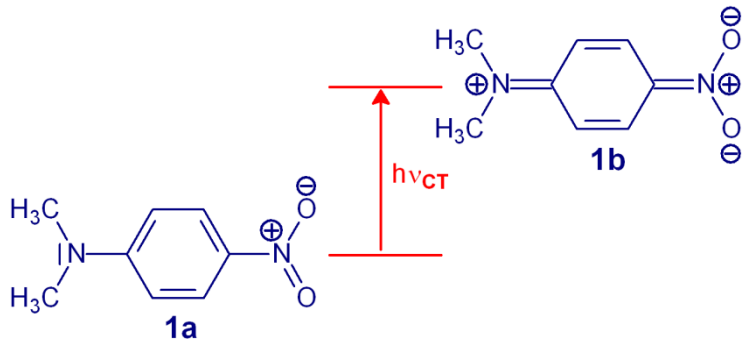

Scheme 1. Charge transfer (CT) optical transition in *N,N*-dimethyl(4-nitro)-aniline (DMNA).

The optical transition is therefore defined charge transfer (CT) transition, characterized by an intense absorption band in the visible region (λ_{max} = 390 nm, ε = 20600 M^{-1} cm^{-1}, EPA, 77K). The highly polar nature of the excited state accounts for the distinctive solvatochromic behaviour. The more polar the solvent, the more pronounced the red shift of the absorption band.

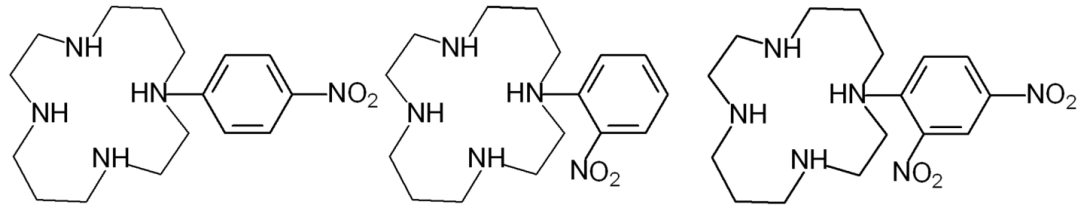

We had previously appended the DMNA subunit to the framework of cyclam and we had observed that the resulting macrocycle **2** was able to incorporate irreversibly and selectively the copper(II) ion.[1] Coordination of Cu^{2+} to the anilino nitrogen atom of **2** makes the intensity of the dipole decrease. As a consequence, the CT band is remarkably blue-shifted (from 386 t0 266 nm) and, on Cu^{II} addition, under diluted conditions (< 10^{-4} M), the yellow-orange solution of **2** turns colourless. Macrocyle **2** can be therefore considered an exclusive optical dosimeter of Cu^{II}.[2] Moreover, structural studies on the $[Cu^{II}(\mathbf{2})](ClO_4)_2$ complex showed that the Cu^{2+} ion is fully encircled by the macrocycle according to a square geometry.[1]

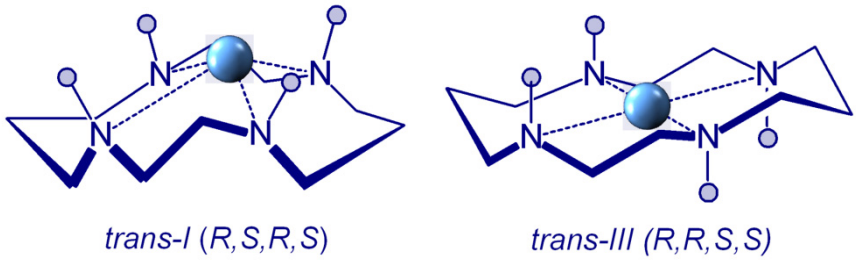

Scheme 2. *Trans-I* and *trans-III* configurational isomers of metal cyclam complexes.

Quite interestingly, the macrocycle adopts the *R,S,R,S* configuration (diastereoisomer *trans-I*, see Scheme 2), rather unusual for metal complexes of mono-substituted cyclam derivatives and typically observed with metal complexes of *N,N',N'',N'''*-tetrasubstituted cyclams.[3] On the other hand, unsubstituted or mono *N*-substituted cyclam complexes usually adopt an *R,R,S,S* configuration (*trans-III*) (see Scheme 2).[4]

We wish now to extend the study to the copper(II) complexes of cyclam derivatives with a 2-nitrophenyl (**3**) and with a 2,4-dinitrophenyl substituent (**4**). This could allow us to evaluate (i) how Cu^{II} coordination modifies the properties of the push-pull chromophore and (ii) if the 2-nitro group can bind the metal center from the top, according to a scorpionate mode. Factors affecting the coordination of the nitro group have been elucidated thanks to the determination of the crystal and molecular structures of seven complex salts of macrocycles **2**, **3** and **4**. They are the only structures available for metal complexes of cyclam derivatives with a nitrobenzyl substituent directly linked to a nitrogen atom, along with the precursor complex described in ref. (1). Noticeably, the $–NO_2$ group had been observed to coordinate the Cu^{II} ion only in the nitronate form, in a macrocycle in which the 2-nitrophenyl fragment was appended through an ethylenic chain to a nitrogen atom of cyclam.[5]

■ RESULTS AND DISCUSSION

Macrocycles 2, 3 and 4 as specific dosimeters of copper(II). Figure 2 shows the absorption spectra in MeCN of the three macrocycles **2**, **3** and **4**.

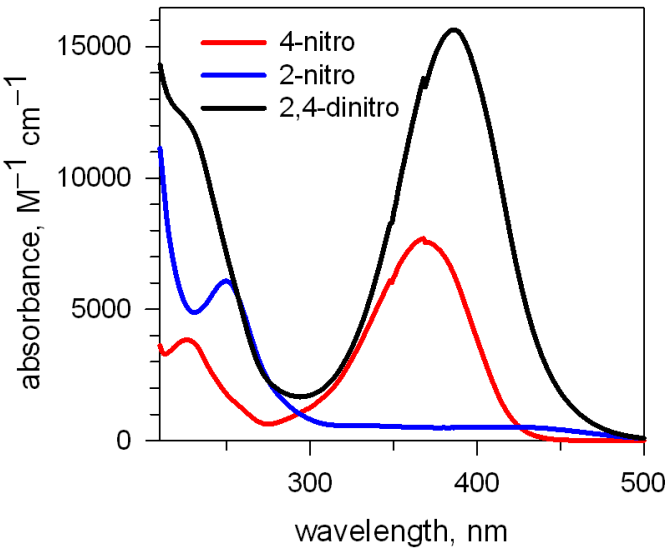

Figure 1. Absorption spectra of macrocycles **2** (4-nitro in the legend), **3** (2-nitro) and **4** (2,4-dinitro) taken in MeCN solution, at 25 °C.

Macrocycles **2** (nitrophenyl substituent in *para*-, yellow-orange color)) and **4** (nitrophenyl substituents in *ortho*- and *para*-, orange) show an intense absorption band at 365 nm (ε = 7950 M^{-1} cm^{-1}) and at 382 nm (ε = 15900 M^{-1} cm^{-1}), respectively, which can be ascribed to the CT transition illustrated in Scheme 1. Such a band is absent for the macrocycle **3**, which does not bear a nitrophenyl substituent in 4 and shows a pale yellow color.

Macrocycles **2** and **4**, in MeCN solution, uptake one Cu^{II} ion to give a substitutionally inert complex, from which the metal ion cannot be extruded even under drastic conditions (addition of excess of competing ligands, of strong acid). Figure 2a shows the spectra taken over the course of the titration of an MeCN solution of **4** with Cu^{II}. Complexation induces a substantial blue-shift of the absorption band assigned to the CT transition from the anilino group to the 4-nitro substituent (from 385 nm to 280 nm), a behavior previously observed also in the case of derivative **2** (blue-shift from 365 nm to 260 nm, in MeCN)).[1]

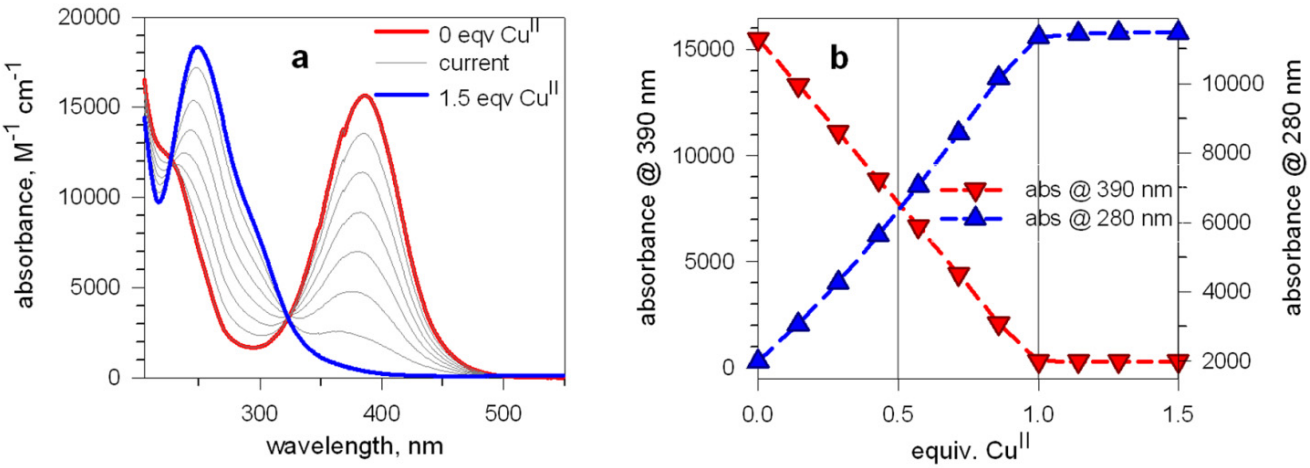

Figure 2. (a) Family of spectra taken over the course of the titration of an MeCN solution of **4** with a standard MeCN solution of $Cu^{II}(CF_3SO_3)_2$; (b) titration profiles (absorbance vs. equiv. of Cu^{II}) at 390 nm and 280 nm), indicating the formation of a complex of 1:1 stoichiometry.

The nature of the blue-shift is illustrated in Figure 3, where the 4-nitrophenyl derivative is specifically considered. It is suggested that the excited state of the Cu^{II} complex is highly destabilized due to the formal electrostatic repulsion between the metal ion and the anilino nitrogen atom, made positive by the charge transfer (see Fig. 3b). This makes $h\nu_{CT}$ distinctly larger than observed for the uncomplexed macrocycle (Fig. 3a).

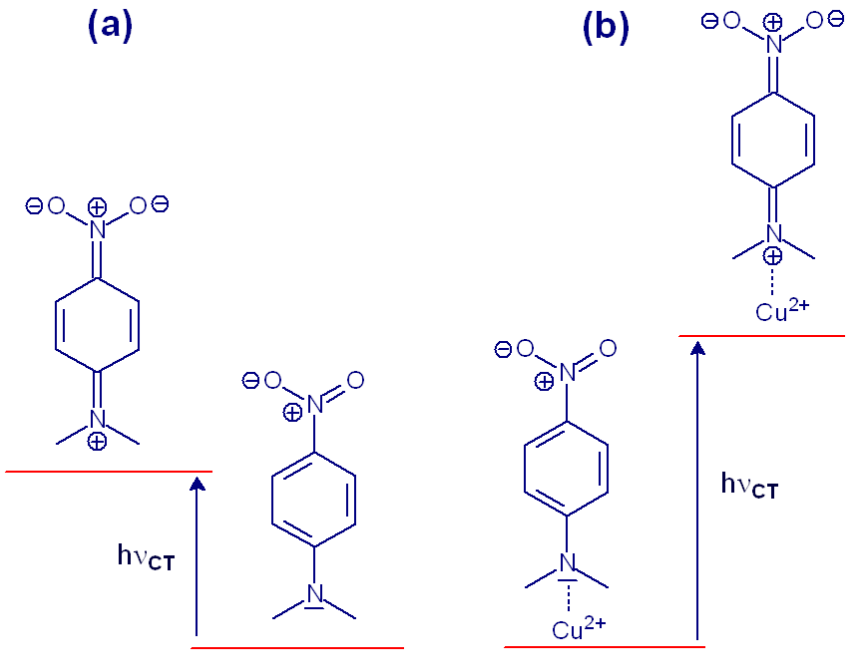

Figure 3. Energy diagrams illustrating the charge transfer transitions in (a) the uncomplexed macrocycle **2**, and (b) macrocycle **2** incorporating Cu^{II}.

Titration profiles at selected wavelengths, shown in Figure 2b, indicate the 1:1 stoichiometry of the complex formed in MeCN. Addition of any other divalent 3d metal to an MeCN solution of **4** did not cause any spectral modification. Thus, receptor **4** appears as a specific dosimeter for Cu^{II}, in the same way as the mono-nitro derivative **2**, but displaying a higher sensitivity due to the higher intensity of the absorption band. The substantial blue-shift makes the yellow diluted solution of the

macrocycle (< 10^{-4} M) turn colorless. A yellow to red color change is observed at a higher concentration (≥ 10^{-3} M), due to the significant appearance of *d-d* bands (*vide infra*).

Complexation of Cu^{II} by the 2-nitro derivative **3** in MeCN causes a distinctly different behavior. Figure 4a shows the family of spectra taken over the course of the titration of a MeCN solution of **4** with a standard MeCN solution of $Cu^{II}(CF_3SO_3)_2$.

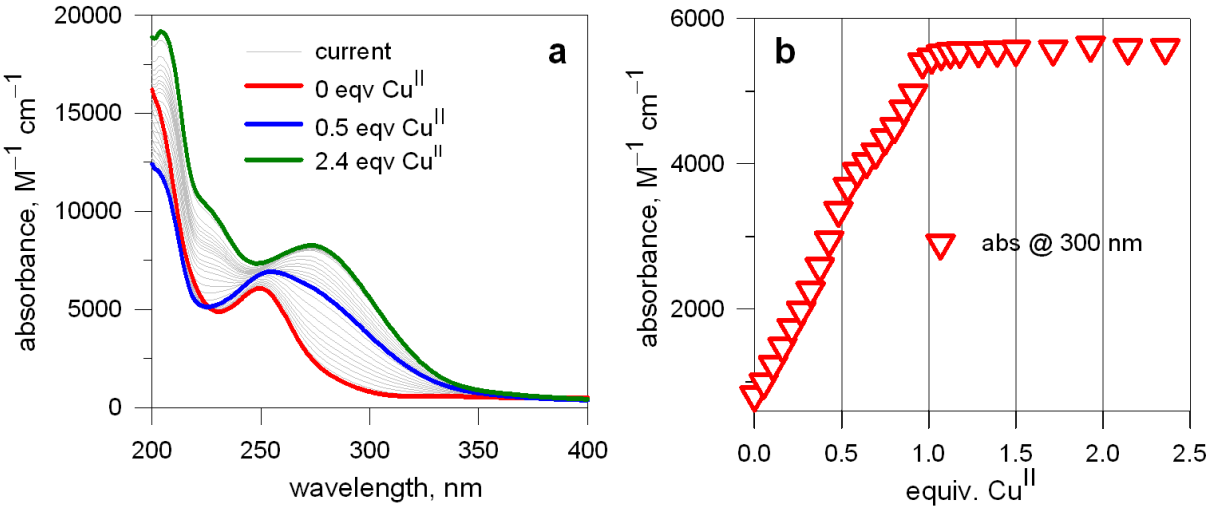

Figure 4. (a) Family of spectra taken over the course of the titration of an MeCN solution of **2** with a standard MeCN solution of $Cu^{II}(CF_3SO_3)_2$; (b) titration profiles (absorbance vs. equiv. of Cu^{II}) at 300 nm), which monitors the formation of the 1:1 metal complex..

It is observed that metal complexation provokes a moderate, still distinct red shift of the band ed at 250 nm (shifted to 275 nm on addition of excess Cu^{II}). The nature of the red-shift is tentatively illustrated in Figure 5.

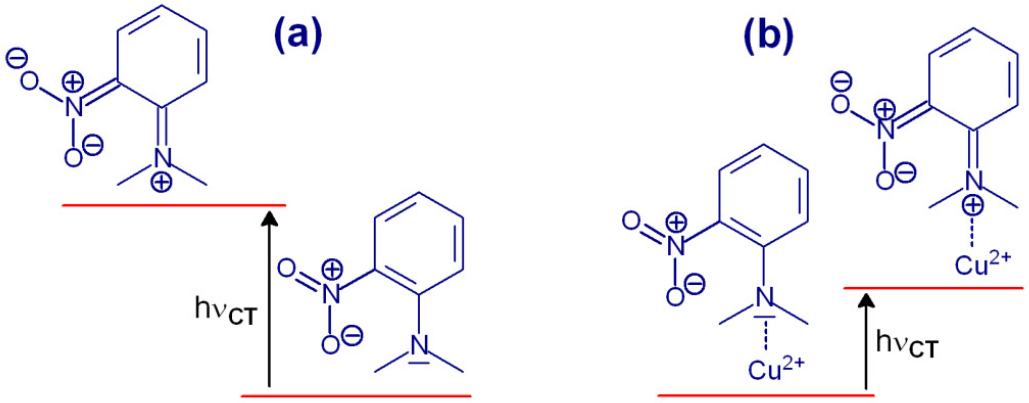

Figure 5. Energy diagrams illustrating the charge transfer transitions in (a) the uncomplexed macrocycle **3**, and (b) macrocycle **3** incorporating Cu^{II}.

In particular, the excited state of the metal complex (part b of the Figure) may be stabilized by the attractive electrostatic interaction between one negatively charged oxygen atom of the nitronate group on one side and (i) the close iminium group, and (ii) the Cu^{2+} ion, on the other.These interactions cannot be established when the nitro substituent is in *ortho*- position.

The titration profile shown in Figure 4b clearly indicates the incorporation of copper(II) ion by the macrocycle according to a 1:1 stoichiometry. Also in the present case, metal uptake is

irreversible, thus defining **3** as an optical dosimeter of Cu^{II}. It should be noted that in the titration profile at 300 nm in Fig. 5b a discontinuity exists at the addition of 0.5 equiv. of Cu^{II}. Such a feature could be tentatively ascribed to the formation of an intermediate species of 1:2 metal/ligand ratio, in which each macrocycle molecule contributes to the coordination with 2 (or 3) primary nitrogen atoms.

Conformational aspects: the existence of a scorpionate effect. On preparation of crystalline metal complexes salts of macrocycles **3** and **4** products of different color were obtained depending upon the chosen experimental conditions. The structural features of the different complex salts were clearly defined through single crystal X-ray diffraction studies.

Complexes of 4. On addition of an MeOH solution of copper(II) perchlorate (pale blue) to an MeOH solution of **4** (yellow) a red precipitate formed, while the supernatant solution took a violet color. Red crystals suitable for X-ray diffraction studies were obtained on diffusion of diethylether vapor on an MeCN solution of the red solid. The crystal and molecolar structure of the $[Cu^{II}(\mathbf{4})](ClO_4)_2$ complex salt is shown in Figure 6.

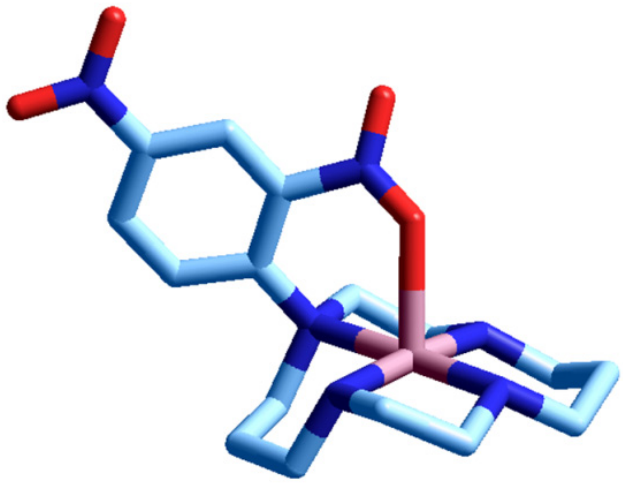

Figure 6. The crystal and molecular structure of the complex salt *trans-I*-$[Cu^{II}(\mathbf{4})](ClO_4)_2$, red color. Hydrogen atoms and counteranions, not involved in metal coordination, have been omitted for clarity.

The complex is five-coordinate, according to a square pyramidal geometry: the four amine nitrogen atoms of the macrocycle occupy the corners of the square, while an oxygen atom of the nitro group in *ortho* position of the phenyl substituent occupy the apical site. The cyclam framework exhibits a *trans-I* configuration. The presence of a tertiary nitrogen atom in the cyclam framework induces some distortion in the coordination polyhedron: (i) the $Cu^{II}–N_{tert}$ distance is 214(1) pm vs the 199(1)-200(1) pm $Cu^{II}–NH$ distances (while the $Cu^{II}–O$ distance is 233(1) pm) , (ii) the $O–Cu^{II}–N_{tert}$ angle is 80.7(1)°.

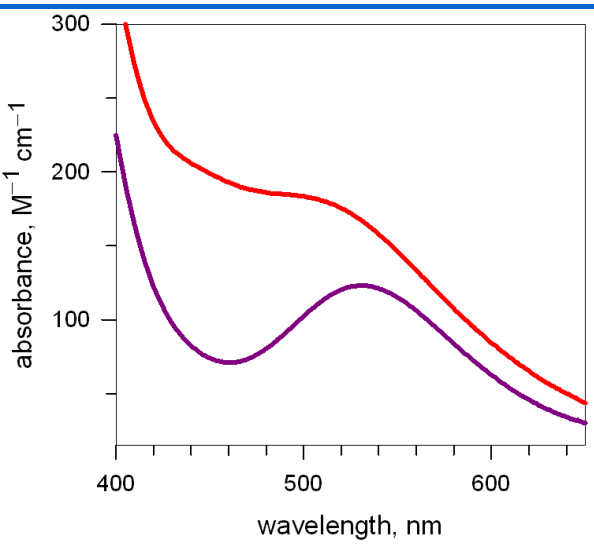

Figure 7. Red line: spectrum of an MeCN solution of the red form of the $[Cu^{II}(\mathbf{4})](ClO_4)_2$ complex salt (*trans-I* configuration); violet line: spectrum of the same solution taken after several weeks.

On dissolution of the red complex salt *trans-I-*$[Cu^{II}(\mathbf{4})](ClO_4)_2$ in MeCN, a red solution is obtained, whose absorption spectrum is shown in Figure 7 (red solid line). The red solution turns violet over a period of weeks. The spectrum of the solution, taken when no further modifications were observed, is shown in Figure 7 (violet solid line). On slow evaporation of the violet solution, the violet complex salt $Cu^{II}(\mathbf{4})(ClO_4)_2$·MeCN was obtained in a crystalline form, whose molecular structure was determined through X-ray diffraction studies. The corresponding structure is shown in Figure 8.

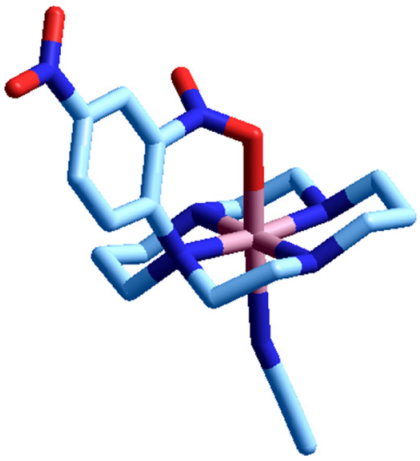

Figure 8. The crystal and molecular structure of the complex salt *trans-III*-$[Cu^{II}(\mathbf{4})(ClO_4)_2$·MeCN], violet color. Hydrogen atoms and counteranions, not involved in metal coordination, have been omitted for clarity.

The complex shows an elongated octahedral geometry, with a scorpion type coordination of the nitro group in the pheyl *ortho* position and the nitrogen atom of an MeCN molecule occupying the opposite axial position. Noticeably, the cyclam framework exhibits a *trans-III* configuration. Also in the present case, the N4 square is distorted, as the Cu^{II}–N_{tert} distance (215(1) pm) is distinctly higher than the Cu^{II}–NH distances (ranging from 201(1) to 203(1) pm)). The two axial distances are 241(1) and 240(1) pm for Cu^{II}–O and Cu^{II}–N, respectively.

If diethylether vapor is allowed to diffuse on an MeCN solution of the red complex salt $[Cu^{II}(\mathbf{4})](ClO_4)_2$, in the presence of $[Bu_4N]Cl$, blue-violet crystals of the salt $Cu^{II}(\mathbf{4})Cl_2·H_2O·½Et_2O$

form, which were investigated through X-ray diffraction studies. The corresponding crystal and molecular structure is shown in Figure 9.

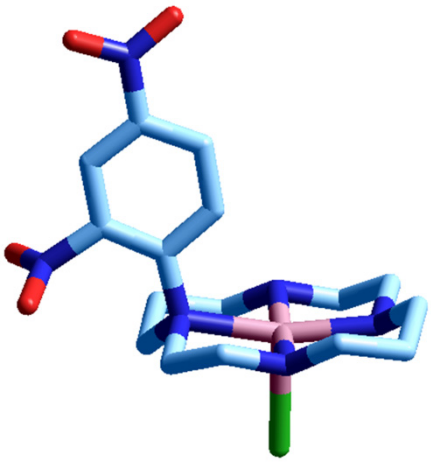

Figure 9. The crystal and molecular structure of the complex salt *trans-III*-[Cu^{II}(**4**)Cl]Cl·H_2O.½$(C_2H_5)_2O$. The chloride counterion, not involved in coordination, as well as solvational molecules have been omitted for clarity.

It is observed that the complex cation [Cu^{II}(**4**)Cl]$^+$ shows a square pyramidal coordination geometry, with the chloride ion occupying the apical position. The nitro group in *ortho* position is well far away from the metal , while the macrocycle adopts the *trans-III* configuration.

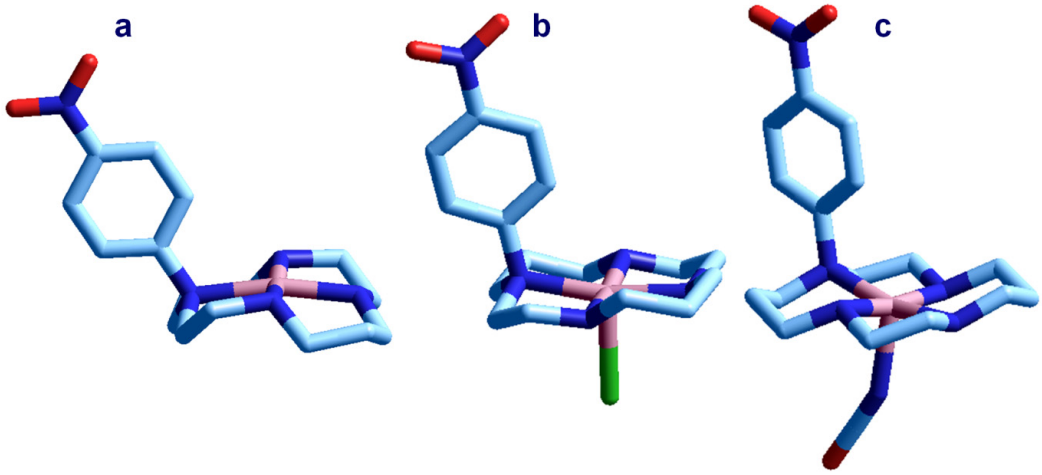

Figure 10. Crystal and molecular structure of the complex salts: (a): *trans-I*-[Cu^{II}(**2**)]$(ClO_4)_2$, red color;[1] (b) 2(*trans-III*-[Cu^{II}(**2**)Cl]Cl)·MeCN·$^5/_2H_2O$, blue color; (c) *trans-III*-[Cu^{II}(**2**)(NCO)]NCO·2(H_2O), blue color. Hydrogen atoms, counterions and solvational molecules have been omitted for clarity. Crystal of **b** contains two similar but not symmetrically equivalent [Cu^{II}(**2**)Cl]$^+$ molecular cations

We have now observed that on diffusion of diethylether on an MeCN solution of *trans-I*-[Cu^{II}(**2**)]$(ClO_4)_2$ in the presence of an excess of [Bu_4N]]X (X = Cl, NCO), the following complex salts can be obtained in a crystalline form, suitable for X-ray diffraction studies: *trans-III*-[Cu^{II}(**2**)Cl]Cl (Figure 10b) and *trans-III*-[Cu^{II}(**2**)(NCO)]NCO·H_2O (Figure 10c). For comparative purposes, Figure 10a shows the crystal and molecular structures of the complex salts of the parent macrocycle **2**: *trans-I*-[Cu^{II}(**2**)]$(ClO_4)_2$ (Figure 10a).[1] It should be noticed that, in the presence of a coordinating anion like Cl^- and NCO^-, the complex moves from the square geometry (**a**) to a square

pyramidal arrangement (**b**, **c**), while cyclam configuration changes from *trans-I* to *trans-III*. In the three complexes, the Cu^{II}–N_{tert} distances remain a bit longer than the Cu^{II}–NH distances. However, the distortions for the N4 squares in the three complexes of **2** are less pronounced than in complex **a**. Actually, the Cu^{II}–N_{tert} distances range from 207(1) pm in the *trans-I* complex (**a**) to 209(1) pm in the *trans-III* complex (**c**), whereas the Cu^{II}–NH distances are in the range 200(1)−204(1) pm. The axial distances are 253(1) and 257(1) pm for Cu^{II}–Cl in the two independent molecules of **b** and 218(1) pm for Cu^{II}–N_{NCO} in complex **c**. Notice that on halide/pseudohalide coordination the Cu^{II} ion, only 3(1) pm over the mean N4 plane in the *trans-I* complex **a**, is raised by 18(1)/23(1) pm from the plane towards the anion, respectively.

On the basis of the structural data described above, the following conclusions can be drawn:

1. The presence of the hindering phenyl substituent favors the *trans-I* configuration.
2. Coordination of a further ligand (an anion, an MeCN molecule, the oxygen atom of the nitro group) favors the conversion to the *trans-III* configuration: the higher the coordinating tendencies of the exotic ligand, the easier the *trans-I* to *trans-III* conversion.

Thus, whatever the position the nitro group is, whether *ortho-* or *para-*, the kinetically less complicated pathway leads to the formation of a complex in a *trans-I* configuration. In the case of the complex of macrocycle **4**, the five-cordinate scorpionate complex forms. However, this is not the thermodynamically stable species and the *trans-I* scorpionate species (red) slowly converts in MeCN to the octahedral scorpionate *trans-III* form (violet), with an MeCN molecule occupying the axial position opposite to the coordinated oxygen atom of the nitro group. If a coordinating anion is present (Cl^-, NCO^-), the *trans-III* complex prefers to bind the anion according to a square pyramidal geometry, diverting the $–NO_2$ oxygen from the axial site and releasing the bound MeCN molecule to the solution. The metal profits at most from the anion coordination by raising itself 19(1) pm from the N4 plane (a behavior observed also with complexes of **2** with chloride and cyanate).

Complexes of 3. Red solvate complex salt $[Cu^{II}(\mathbf{3})](ClO_4)_2 \cdot MeCN$ and violet complex salt $[Cu^{II}(\mathbf{3})](ClO_4)_2$ were obtained through reaction of $Cu(ClO_4)_2$ with **3** in MeCN in the same crop. *Trans-I* and *trans-III* complex were separated by elution through a cation exchange column. The crystal and molecular structures of the two forms are shown in Figure 11.

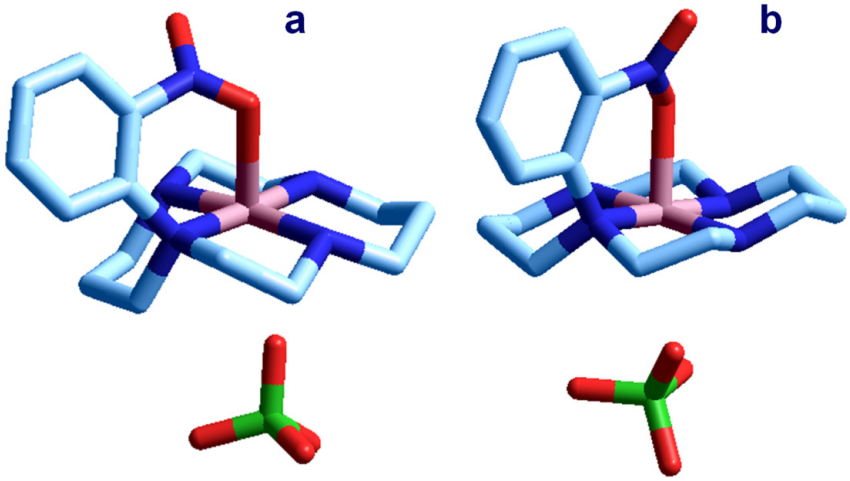

Figure 11. Crystal and molecular structure of the complex salts: (a) : *trans-I*-$[Cu^{II}(\mathbf{3})](ClO_4)_2 \cdot MeCN$, red color; and (b) *trans-III*-$[Cu^{II}(\mathbf{3})](ClO_4)_2$, violet color. Hydrogen atoms unbound perchlorate ions and solvational molecules have been omitted for clarity.

As noted for **4**, the red form corresponds to the *trans-I* configuration of the cyclam macrocycle, while the violet complex shows the *trans-III* arrangement. In contrast to what observed for the analogous complexes of **4**, crystals of the red *trans-I*-$[Cu^{II}(\mathbf{3})]^{2+}$ complex contain an MeCN molecule, which is not bonded to the metal , whereas the violet *trans-III* $[Cu^{II}(\mathbf{3})]^{2+}$ species does not keep in the solid state any MeCN molecule. In particular, the apical site opposite to the coordinated nitro group of both *trans-I* and *trans-III* Cu^{II} complexes of **3** is occupied by a perchlorate anion, whose loosely bound oxygen atom is positioned at 277(1) pm for *trans-I* $[Cu^{II}(\mathbf{3})]^{2+}$ species and 272(1) pm for *trans-III* $[Cu^{II}(\mathbf{3})]^{2+}$ species.

Other structural features are in full agreement with the principles outlined in the previous Section. In particular, both *trans-I* and *trans-III* complexes of **3** show Cu^{II}–N_{tert} distances (210(1) and 209(1) pm) longer than the Cu^{II}–NH distances (in the range 199(1)-203(1) pm). The axial Cu^{II}–O distances are 236(1) pm and 224(1) pm in *trans-I* $[Cu^{II}(\mathbf{3})]^{2+}$ and *trans-III* $[Cu^{II}(\mathbf{3})]^{2+}$ complexes, respectively.

Mechanism of the *trans-I* to *trans-III* conversion. It has been mentioned that the *trans-I* complex of both **3** and **4** macrocycles slowly and spontaneously converts in solution to the thermodynamically stable *trans-III* complex, which keeps a scorpionate arrangement. Figure 7 has shown that the two configurational isomers exhibit well distinct spectral features in the *d-d* region of the absorption spectrum, which allows their detection in solution. Thus, the kinetic aspects of the *trans-I* to *trans-III* conversion could be investigated spectrophotometrically.

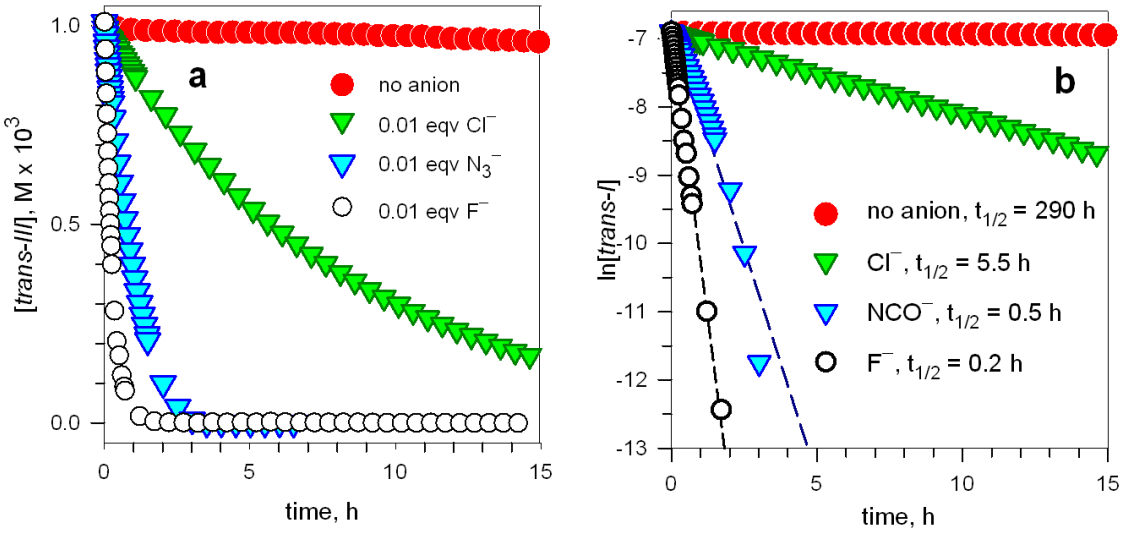

Figure 12. Kinetic studies on the *trans-I* to *trans-III* conversion of the *trans-I* $[Cu^{II}(\mathbf{3})](ClO_4)_2$ complex in an MeCN solution at 25°C (10^{-3} M). The decay of the *trans-I* complex concentration is monitored through the decrease of the absorbance of the absorption band at 460 nm: (a) conversion in the absence of anions and in the presence of a catalytic amount of a $[Bu_4N]X$ salt (10^{-5} M, $X^- = Cl^-$, NCO^-, F^-); (b) ln[*trans-I*] vs. time plots, disclosing a first-order behavior.

Figure 12a shows the decay of the concentration of the *trans-I* complex (red filled circles), which has been calculated from the absorbance at 460 nm, corrected for the absorbance of the *trans-III* complex, of an MeCN solution 10^{-3} M in the *trans-I* $[Cu^{II}(\mathbf{4})](ClO_4)_2$ complex salt (red color, values at larger times not reported in the diagram). In Figure 12b, ln[*trans-I*] has been plotted vs. time (h). The linear behaviour indicates the first-order nature of the process, to which a half-time $t_{1/2}$ ~ 12 days corresponds.

The presence of anions in catalytic amounts (i.e. 10^{-5} M) makes the *trans-I*-to-*trans-III* conversion considerably faster. In this connection, Figure 12a shows the decay of the absorbance at 460 nm for an MeCN solution 10^{-3} M in $[Cu^{II}(\mathbf{4})]^{2+}$ and 10^{-5} M in $[Bu_4N]Cl$. The linear ln[*trans-III*] vs. t(h) in Figure 12b discloses a $t_{1/2}$ = 5.5 h. We can tentatively suggest that the *trans-I* to *trans-III* conversion may take place through a dissociative mechanism (detachment of an amine nitrogen atom, as a preliminary step to the configurational reorganization). The chloride ion is assumed to temporarily occupy the empty coordination site, thus decreasing the energy of the transition state. Accordingly, anions of higher coordinating tendencies than chloride should make the conversion process faster. Indeed, in the presence of 1/100 equiv. of cyanate, which follows chloride in the spectrochemical series, the rate the configurational rearrangement increases distinctly and the half-time is substantially reduced ($t_{1/2}$ = 0.5 h).

It is therefore surprising that the highest acceleration is exerted by the less cordinating halide ion, fluoride (see empty circles in Figure 12a), to which a half-time $t_{1/2}$ = 13 minutes corresponds (from the linear plot in Figure 12 b.Such an unexpected behavior has to be related to the Brønsted base properties rather than to the coordinating properties of F^-, as it will be discussed in detail in the next Section.

Base effect on the *trans-I*−to−*trans-III* conversion. An aqueous solution of the *trans-I*-$[Cu^{II}(\mathbf{4})](ClO_4)_2$ complex salt, to which excess strong acid had been added and which had been made 0.1 M in $NaClO_4$, was titrated with a standard solution of NaOH, at 25°C. Figure 13a shows the family of spectra taken during the course of the titration over the 7.0-12.5 pH interval.

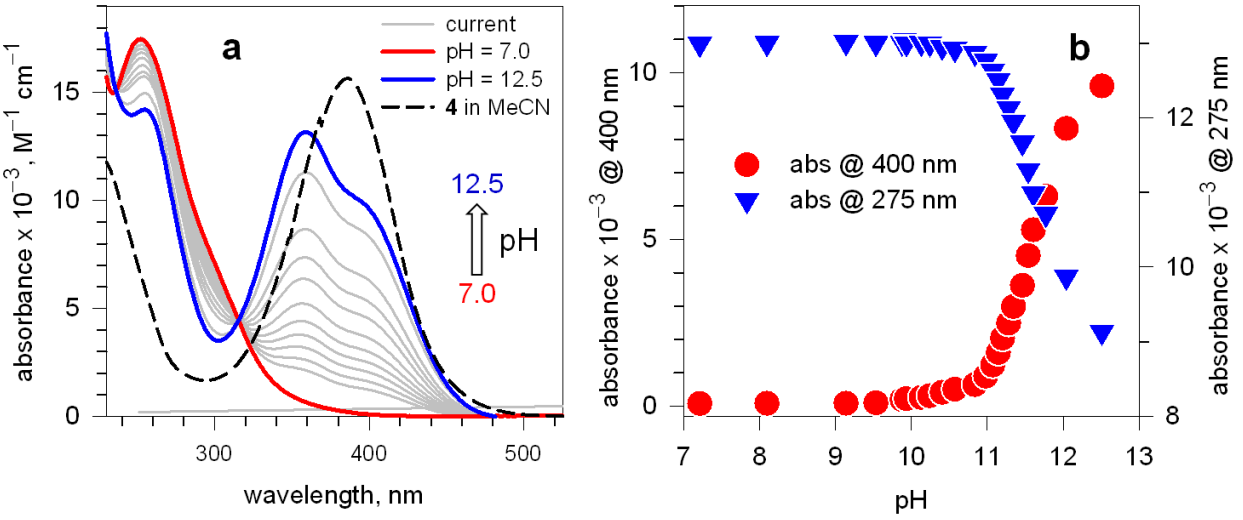

Figure 13. (a) Spectra taken over the course of the titration of an aqueous solution 10^{-4} M in *trans-I*-$[Cu^{II}(\mathbf{4})](ClO_4)_2$ and 0.1 M in $NaClO_4$; (b) titration profiles based on the decreasing absorbance at 275 nm, monitoring the concentration of the $[Cu^{II}(\mathbf{4})]^{2+}$ complex (blue triangles, right vertical axis) and the increasing absorbance at 400 nm, due to the demetalated-deprotonated macrocyle **4** (red circles, left vertical axis).

It is observed that at pH ≥ 10 the absorbance of the band at 275 nm, pertinent to the $[Cu^{II}(\mathbf{4})]^{2+}$ complex, decreases according to a sigmoidal profile. At the same pH a new band develops, ed at 360 nm, with a well defined shoulder at 400 nm, still showing a sigmoidal profile. It is hypothesized that $[Cu^{II}(\mathbf{4})]^{2+}$ (= $[Cu^{II}(HL)]^{2+}$), behaves as a monoprotic acid, according to the equilibrium (1), which involves simultaneous demetalation:

$$[Cu^{II}(HL)]^{2+} + OH^- \leftrightarrows L^- + Cu^{2+} + H_2O \quad (1)$$

From the two intersecting curves in Figure 13b a value of pK_a ~ 11.8 can be roughly estimated. Thus, the band ed at 360 nm with a shoulder at 400 nm should pertain to the deprotonated macrocycle L^- (HL = **4**) In Figure 13a, the spectrum of the metal-free macrocycle **4** (HL) in MeCN is also displayed for comparative purposes (dotted black line), which originates from one single transition. The fact that the absorption at a pH ≥ 10 results from two distinct transitions suggests that the L^- form exists as an equilibrium mixture of two species, probably differing for the position of the deprotonated amine group, whether closer or farther from the phenylamine nitrogen atom. To the two isomeric species, dipoles of different intensity correspond, as well as transitions of different energy.

The occurrence of demetalation in a strongly basic solution was demonstrated by the following experiment: an aqueous solution of the the *trans-I*-[Cu^{II}(**4**)]$(ClO_4)_2$ complex salt was brought to pH = 14 with NaOH; the yellow solution was then extracted with $CHCl_3$, to which the yellow color was transferred. One drop of the $CHCl_3$ layer was dissolved in MeOH and the ESI mass of the solution was determined: a peak m/z 367.2 ($M+H^+$, 100%) was observed; no peaks with the typical isotopic pattern of Cu^{II} were detected.

Then, we titrated a 10^{-3} M solution of the *trans-I*-[Cu^{II}(**4**)]$(ClO_4)_2$ complex salt in MeCN with a solution of $[Bu_4N]F$ in MeCN. The recorded family of spectra is shown in Figure 14a.

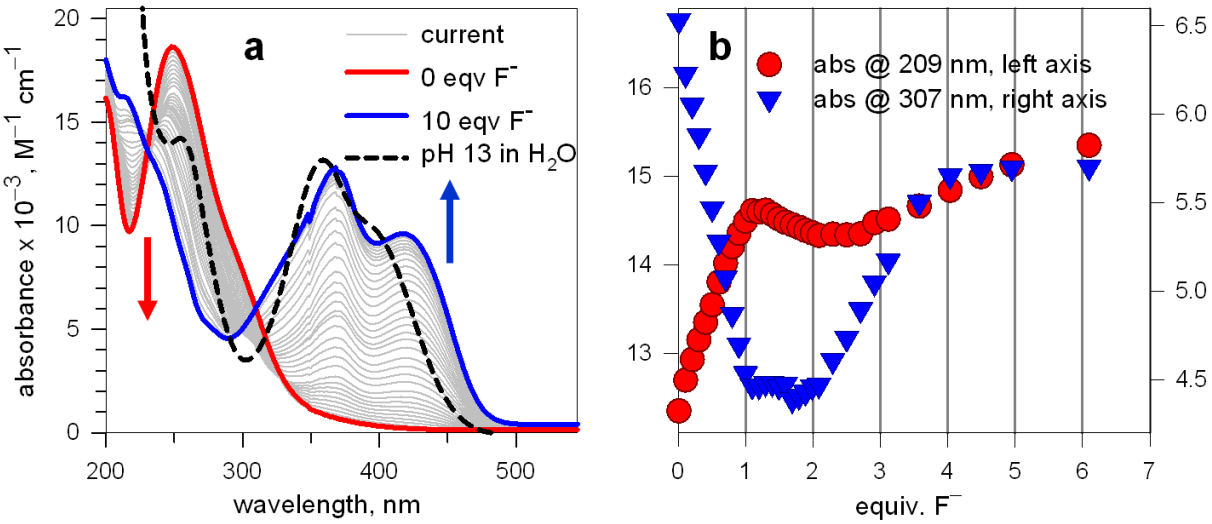

Figure 14. (a) Family of spectra recorded over the course of the titration of a 10^{-4} M solution of the *trans-I*-[Cu^{II}(**4**)]$(ClO_4)_2$ complex salt in MeCN with a solution of $[Bu_4N]F$ in MeCN (optical path 1 cm); (b) titration profiles at selected wavelengths, illustrating the occurrence of a two-step process, at 1 and 2 equiv. of added fluoride.

It is observed that on fluoride addition the band ed at 250 nm, corresponding to the copper(II) complex, decreases in intensity, while a new two-transition band develops at 350-450 nm. Such a band reaches a limiting intensity on addition of excess of fluoride and its shape is strongly reminiscent of that observed in a strongly basic aqueous solution and pertaining to the deprotonated macrocycle L^- (reported as a black dotted line in Figure 14a for comparative purposes). In particular, the band in the visible region shows two well distinct transitions at 360 and 430 nm. Thus, the F^- ion in the MeCN solution acts as a strong base, taking one proton from an N−H group of the macrocycle and inducing demetalation. However, the stoichiometry of the process is not straightforward. In particular, titration profiles at different wavelengths (e.g. at 209 and 307 nm, see Figure 14b) indicate discontinuity after the addition of 1 equiv. and of 2 equiv. of F^-, suggesting the

occurence of a two-step process. In particular, it is proposed that in the 1st step the fluoride ion coordinates the metal to give a five-coordinate complex, analogous to the $[Cu^{II}(\mathbf{4})Cl]^+$ species, whose structure is illustrated in Figure 9. In the 2nd step, deprotonation of one N−H fragment of the macrocycle takes place with formation of the HF_2^- hydrogen bonding complex and demetalation. The two equilibria are described below:

$$[Cu^{II}(HL)]^{2+} + F^- \leftrightarrows [Cu^{II}(HL)F]^+ \qquad (2)$$

$$[Cu^{II}(HL)F]^+ + F^- \leftrightarrows Cu^{2+} + L^- + HF_2^- \qquad (3)$$

In fact, if one F^- ion in an aprotic solvent is not an especially strong base, two F^- ions exert a strongly basic behavior due to the formation of the hydrogen bonding complex HF_2^-, for which the highest HB energy in the gas phase has been determined (38.6 kcal mol^{-1}).[6] Fluoride induced deprotonation of an acidic N−H fragment had been previously observed in the case of urea derivatives (BH),[7-10] when investigated as anion receptors, according to the two stepwise equilibria reported below:

$$BH + F^- \leftrightarrows [BH\cdots F]^- \qquad (4)$$

$$[BH\cdots F] + F^- \leftrightarrows B^- + HF_2^- \qquad (5)$$

First, the hydrogen bonding complex $[BH\cdots F]^-$ forms, eq. (4), then, on addition of the second fluoride ion, deprotonation of one N−H urea fragment takes place, according to an equilibrium displaced to the right by the formation of HF_2^-, eq. (5).[11]

This may explain the strong acceleration of the *trans-I*-to-*trans-III* conversion induced by a catalytic amount of fluoride (see Figure 12). In fact, it may happen that traces of fluoride provoke deprotonation of a microscopic amount of the complex, inducing demetalation, conformational rearrangement, new protonation and new metal complexation. At this stage, the fluoride ion can begin a new cycle.

The spectrophotometric titration experiment illustrated in Figure 14, carried out in a cuvette of 1 cm optical pathway, was also carried out in a cuvette of 10 cm optical path in order to detect spectral changes in the visible region and monitor the occurrence of *d-d* transitions.

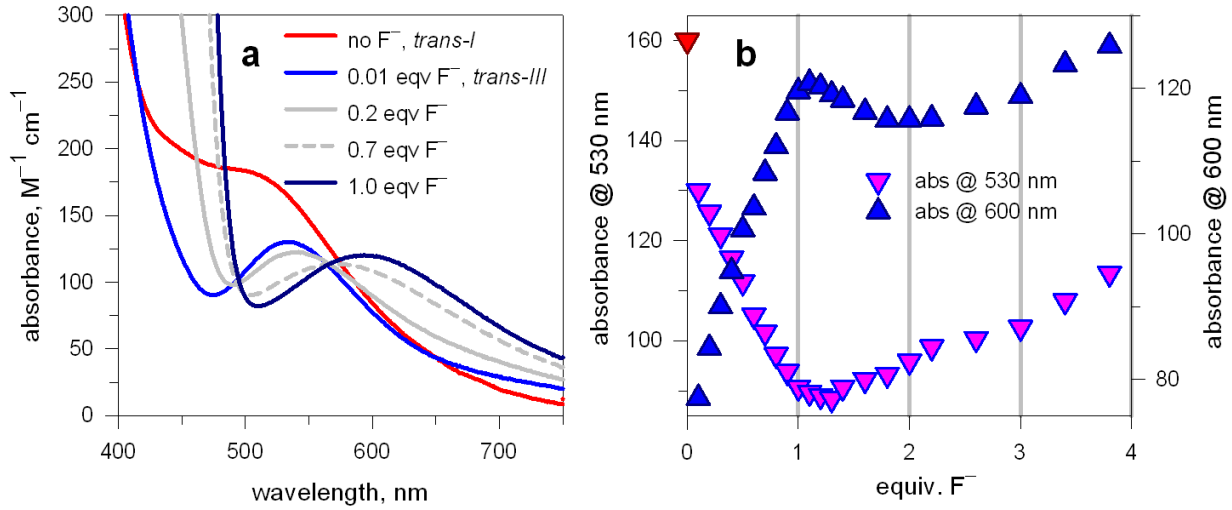

Figure 15. (a) Spectra recorded over the course of the titration of a 10^{-4} M solution of the *trans-I*-$[Cu^{II}(\mathbf{4})](ClO_4)_2$ complex salt in MeCN with a solution of $[Bu_4N]F$ in MeCN (optical path 10 cm); addition of 0.01 equiv. of F^- to the red solution favors the quick formation of the *trans-III* complex and the solution

turns violet; (b) titration profiles at selected wavelengths; the red triangle on the left vertical axis pertains to the *trans-I* complex prior the addition of F^-.

The red dotted line in Figure 15a indicates the spectrum of the solution before anion addition and corresponds to the red *trans-I*-$[Cu^{II}(HL)]^{2+}$ complex. On addition of 0.1 equiv. of F^-, a substantial spectral change quickly takes place and the spectrum indicated by the pink line forms: this is the spectrum of the *trans-III*-$[Cu^{II}(HL)]^{2+}$ complex, whose formation has been made fast by the presence of 0.1 equiv. of fluoride. Further substoichiometric additions of F^- induced a steady red-shift of the *d-d* band, as typically observed on axial coordination of an additional ligand to a copper(II)-tetramine square complex. The process can be followed through the absorbance profiles shown in Figure 15b. The decrease of the absorbance at 530 nm corresponds to the disappearance of the *trans-III*-$[Cu^{II}(HL)]^{2+}$ scorpionate complex, while the increase at 600 nm is related to the formation of the *trans-III*-$[Cu^{II}(HL)F]^{+}$ species of presumably square-pyramidal geometry. However, after the addition of 1 equiv. of anion, a neat discontinuity of the two profiles is observed, due to the incipient decomposition of the macrocyclic complex. A completely similar behavior has been observed with the corresponding non-scorpionate complex of macrocycle **2** (see Supplementary Information).

■ CONCLUSION

It has been shown that appending of a nitrophenyl substituent at a nitrogen atom seriously modifies the spectral properties of cyclam and of its copper(II) complexes. In particular, nitrophenylcyclam derivatives **2** and **4**, containing a nitro group in *para-* position, in an MeCN solution incorporate Cu^{II} according to an irreversible process signaled by a neat color change (yellow-to-red), associated to a significant blue-shift of the charge transfer band. For macrocycle **3**, whose nitro substituent is positioned in *ortho-*, copper(II) incorporation results in a red-shift response. In any case, all the investigated nitrophenylcyclam derivatives accumulate the dose and should be considered *colorimetric dosimeters*. They are specific for copper(II) as they do not complex any other metal ion under the same conditions, at room temperature.

When in the *ortho-* position of the phenyl substituent (macrocycles **3** and **4**), the nitro group can apically coordinate the Cu^{II} ion, according to a scorpionate mode. Nitro coordination influences the configuration of the cyclam-like macrocycle. In fact, the $[Cu^{II}(\mathbf{2})]^{2+}$ complex (one nitro group in *para-*, scorpionate coordination prevented) is obtained in the *trans-I* form, a configuration which is indefinitely maintained. The *trans-III* form is obtained only in the presence of stoichiometric amount of coordinating anions (e.g. Cl^-), with formation of a square-pyramidal complex. The Cu^{II} complex of **4** (one nitro group in *ortho-*) is obtained as a perchlorate salts a scorpionate in a *trans-I* configuration, which slowly converts to the *trans-III* arrangement, maintaining the apical coordination of the nitro fragment. The conversion is dramatically accelerated by catalytic amounts of Cl^-, NCO^- and F^-. While for Cl^- and NCO^- the effect can be associated to the capability of the anion to stabilize through coordination any dissociative intermediate, the very powerful effect exerted by F^- seems to be related to the deprotonation of one N−H fragment of the macrocycle, driven by the formation of the highly stable HF_2^- complex ion.

This work was undertaken in order to design specific and irreversible receptors for Cu^{II}, by coupling the high coordinating tendencies of cyclam and the unique chromophoric properties of the nitrophenyl substituent. While the synthesized ligands display the aimed analytical properties, novel features of interest in basic inorganic and coordination chemistry were discovered, which include

the binding capability of the nitro group according to a scorpionate mode, the factors affecting the thermodynamic and kinetic relative stability of the *trans-I* and *trans-III* configurations of complexed cyclam, the role exerted by the fluoride ion in the deprotonation of a coordinated N−H fragment.

■ EXPERIMENTAL SECTION

Physical measurements. UV/Vis spectra were recorded on a Varian CARY 100 spectrophotometer with quartz cuvettes of the appropriate path lenght (0.1 or 1 cm). In any case, the concentration of the chromophore and the optical path were adjusted in order to obtain spectra with AU ≤ 1. Mass spectra were acquired on a Thermo-Finnigan ion trap LCQ Advantage Max instrument, equipped with an ESI source.

Syntheses. All the macrocycles have been prepared through a multistep synthesis involving a reaction of triprotected cyclam, 1,4,8-tris(*tert*-butoxycarbonyl)-1,4,8,11-tetraazacyclotetradecane (BOC_3cyclam)[1], with the appropriate nitroaryl fluoride, followed by deprotection of the intermediate to yield the desired product. The mono-nitro derivatives **2** (4-nitrophenyl) and **3** (2-nitrophenyl) have been synthesized according to literature procedure,[1,REF] with some modifications, whereas the dinitro derivative **4** (2,4-dinitrophenyl) has been obtained under milder conditions.

*1,4,8-Tris(tert-butoxycarbonyl)-11-(4-nitrophenyl)-1,4,8,11-tetraazacyclotetradecane (**5**)*. A solution of tri-Boc cyclam (2.5 g., 5 mmol) in anhydrous DMSO (30 mL) was added of cesium carbonate (6 g., 18.42 mmol) and heated under stirring to 100 °C under a dinitrogen atmosphere; 1-fluoro-4-nitrobenzene (1.06 mL, 10 mmol) was then added dropwise and the resulting suspension was left to react for 24 hours, added of an additional amount of cesium carbonate (3 g., 9. 12 mmol) and 1-fluoro-4-nitrobenzene (0.53 mL, 5 mmol) and kept until no more increase in the concentration of the product could be detected by MS-ESI (three days). The reaction mixture was left to cool to room temperature and taken up with ethyl acetate (100 mL). The organic solution was then washed with a saturated sodium hydrogencarbonate solution (2 × 30 mL) and brine (1 × 30 mL, left overnight on Na_2SO_4, filtered and evaporated to give an oil. The latter-one was purified through silica gel chromatography (n-hexane/ ethyl acetate 3:2) to give the desired product as a yellow oil (0.99 g., yield: 31.8%), which was satisfactorily characterized through mass spectroscopy (ESI (CH_3OH): m/z 623,4 ($M+H^+$, 100%) and used as such for the following step.

*1-(4-nitrophenyl)-1,4,8,11-tetraaza-cyclotetradecane (**2**).* **5** (0.99 g, 1.6 mmol) was dissolved in dichloromethane (17 mL) and trifluoroacetic acid (1.7 mL) was added dropwise. The solution was stirred at room temperature under a dinitrogen atmosphere until the reaction was complete (~ 20 hours, checked by MS-ESI). The solvent was then removed under *vacuum* to give a dark yellow precipitate, which was dissolved in 5 mL of ethyl acetate and then precipitated with diethylether (75 mL). The solid (a trifluoroacetate adduct) was separated through filtration, taken up with dichloromethane (20 mL) and washed with an equal volume of aqueous NaOH 5%. The organic solution was kept overnight on Na_2SO_4, filtered, and brought to dryness under *vacuum* to give the pure macrocycle **2** (0.45 g., yield: 88.24%). MS (CH_3OH, ESI): m/z 322,2 ($M+H^+$, 100%).

*1-(2-nitrophenyl)-1,4,8,11-tetraaza-cyclotetradecane (**3**).* The synthetic procedure is same as described above for macrocycle **2**, the only difference being the replacement of cesium carbonate with potassium carbonate. Thus, the reaction of tri-Boc cyclam (2.5 g, 5 mmol) in anhydrous DMSO (30 mL) with potassium carbonate (2.6 g., 18.8 mmoli) and 1-fluoro-2-nitrobenzene (1.06 mL, 10 mmol) at 100 °C for three days (including a further addiction of potassium carbonate, 1.3 g.

and 1-fluoro-2-nitrobenzene, 0.53 mL) followed by workup and chromatographic separation (silica gel, n-hexane/ethyl acetate 3:2, gradient) afforded 1,4,8,11-tris(tert-butoxycarbonyl)-11-(2-nitrophenyl)-1,4,8,11-tetraazacyclotetradecane (1.91 g, 3.1 mmol, yield: 61.4%) as an oil, which solidified on standing. Treatment with trifluoroacetic acid (3.4 mL) in dichloromethane (33 mL) gave the pure product (0.8 g, yield: 81.2%). MS (CH_3OH, ESI): m/z 322,2 ($M+H^+$, 100%).

*1-(2,4-dinitrophenyl)-1,4,8,11-tetraaza-cyclotetradecane (**4**).* A solution of 1-fluoro-2,4-dinitrobenzene (0.93 g, 5 mmol) in anhydrous THF (50 mL) was added dropwise to a boiling solution of 1,4,8-Tris(tert-butoxycarbonyl)-1,4,8,11-tetraazacyclotetradecane (2.5 g, 5mmol) and *N,N*-diisopropylethylamine (0.86 mL, 5 mmol) in the same solvent (150 mL). The solution was refluxed under a dinitrogen atmosphere for 24 hours when an additional amount of reagents (0.47 g of 1-fluoro-2,4-dinitrobenzene and 0.43 mL of *N,N*-diisopropylethylamine) was added, then left to react for additional 20 h. The solvent and the excess of *N,N*-diisopropylethylamine were removed *in vacuo* and the residue was purified through liquid chromatography (silica gel, ethyl acetate/hexane 1:1, gradient) to give a yellow oil (3 g, 4.49 mmol, yield: 89.8%), which was satisfactorily characterized through mass spectroscopy (ESI (CH_3OH): m/z 668,4 ($M+H^+$, 100%). The tri-BOC derivative was then dissolved in dichloromethane (47 mL), added of trifluoroacetic acid (4.7 mL) and left to react at room temperature until complete removal of the *tert*-butoxycarbonyl groups (~ 27 hours). The volatiles were distilled off under *vacuum* and the residual orange-yellow oil was dissolved in ethyl acetate (40 mL); the resulting solution was then treated with diethyl ether (200 mL) to form a sticky, yellow solid. The solid was taken up with aqueous NaOH 10% (50 mL) to give a mixture which was extracted with toluene (3 × 50 mL). The combined organic phases were then washed with water (3 × 50 mL), dried overnight on Na_2SO_4, filtered and distilled to dryness under *vacuum* to give the pure product (0.95 g., 2.58 mmol, yield: 57.4%) (ESI (CH_3OH): m/z 369,4 ($M+H^+$, 100%).

Trans-I-[Cu^{II}(**4**)](ClO_4)$_2$. 18.4 mg of **4** (0.0501 mmol) was dissolved in 3 mL of CH_2Cl_2, to which a solution of 18.2 mg (0.0491 mmol) of $Cu(ClO_4)_2 \cdot 6H_2O$ in 0.5 mL of MeCN was added at room temperature. A red brown solution formed, to which 5 mL of diethylether were added. A dark-brown gummy precipitate formed, which was suspended in 1 mL of MeOH and sonicated. A red-orange powder formed, which was filtered on a Hirsch funnel, washed with iced MeOH, dried and recrystalized from MeCN through slow diffusion of diethylether. Red crystals were obtained (21.8 mg, yield 71%. ESI-MS: m/z 214.5 (M^{2+}).

Trans-III-[Cu^{II}(**4**)](ClO_4)$_2$. Violet crystals suitable for X-ray diffraction studies were obtained by dissolving the red *trans-I*-[Cu^{II}(**4**)](ClO_4)$_2$ complex salt in MeCN (~ 10^{-3} M). Then, 0.01 eqv of [Bu_4N]F was added. The solution was kept at room temperature for 1 d. On slow diffusion of diethylether, violet crystals formed.

Trans-I-[Cu^{II}(**3**)](ClO_4)$_2$ and *Trans-III*-[Cu^{II}(**3**)](ClO_4)$_2$. A similar procedure as for *trans-I*-[Cu^{II}(**4**)](ClO_4)$_2$ was followed. The dark-brown gummy precipitate which formed was charged on a Sephadex SP C-25 column and eluted with aqueuous $NaClO_4$. A red and a violet fraction were separated (the red one eluted first). Slow evaporation at room temperature of the two fractions gave the crystalline materials studied through X-ray diffraction.

Complexes containing chloride and cyanate were obtained through crystallization of MeCN solutions of the *trans-I* perchlorate complex salt in the presence of an excess of the corresponding [Bu_4N]X salt (X = Cl, NCO).

X-ray crystallographic studies. Diffraction data for $[Cu^{II}(\mathbf{4})](ClO_4)_2$ (*trans-I*, red color, 0.43 × 0.32 × 0.22 mm^3), $[Cu^{II}(\mathbf{4})](ClO_4)_2\cdot$MeCN (*trans-III*, violet color, 0.51 × 0.14 × 0.04 mm^3), $[Cu^{II}(\mathbf{4})Cl]Cl\cdot H_2O\cdot{}^1/_2(Et_2O)$ (*trans-III*, blue-violet color, 0.51 × 0.14 × 0.04 mm^3, with disordered diethylether and partly populated atom sites of water solvent molecules), $[Cu^{II}(\mathbf{2})(NCO)]NCO\cdot 2(H_2O)$ (*trans-III*, blue color, 0.62 × 0.40 × 0.11 mm^3, with disordered cyanate and partly populated atom sites of water solvent molecules), $[Cu^{II}(\mathbf{3})](ClO_4)_2\cdot$MeCN (*trans-I*, red color, 0.50 × 0.36 × 0.11 mm^3), and $[Cu^{II}(\mathbf{3})](ClO_4)_2$ (*trans-III*, violet color, 0.65 × 0.43 × 0.07 mm^3) have been collected by means of a conventional Enraf-Nonius CAD4 four circle diffractometer.

Diffraction data for $2([Cu^{II}(\mathbf{2})Cl]Cl)\cdot MeCN\cdot{}^5/_2(H_2O)$ (*trans-III*, blue color 0.28 × 0.12 × 0.10 mm^3, with a disordered acetonitrile molecule) have been collected by means of a Bruker-Axs CCD-based three circle diffractometer. Both instruments work at ambient temperature with graphite-monochromatized Mo-Kα X-radiation (λ = 0.71073 Å).

Data reductions for intensities collected with the conventional diffractometer were performed with the *WinGX* package;[12] absorption effects were evaluated with the ψ-scan method,[13] and absorption correction was applied to the data. Data reduction for frames collected by the CCD-based system was performed with the *SAINT* software;[14] absorption effects were empirically evaluated by the *SADABS* software,[15] and absorption correction was applied to the data. All crystal structures were solved by direct methods (*SIR 97*)[16] and refined by full-matrix least-square procedures on F^2 using all reflections (*SHELXL 97*).[17] Anisotropic displacement parameters were refined for all non-hydrogen atoms, excluding some atom sites partly populated and belonging to disordered solvent molecules. Hydrogens bonded to C atoms were placed at calculated positions with the appropriate AFIX instructions and refined using a riding model; hydrogens bonded to secondary amines of the macrocycle moiety and to water molecules (when possible) were located in the final ΔF maps and their positions were successively refined restraining the N−H or O−H distance to be 0.90 ± 0.01 Å. Crystal data are reported in Table 1.

Table 1. Crystal data for investigated crystals.

	$[Cu^{II}(\mathbf{4})](ClO_4)_2$	$[Cu^{II}(\mathbf{4})](ClO_4)_2\cdot$MeCN	$[Cu^{II}(\mathbf{4})Cl]Cl\cdot H_2O\cdot{}^1/_2(Et_2O)$	$2([Cu^{II}(\mathbf{2})Cl]Cl)\cdot MeCN\cdot{}^5/_2(H_2O)$	$[Cu^{II}(\mathbf{2})(NCO)]NCO\cdot 2(H_2O)$	$[Cu^{II}(\mathbf{3})](ClO_4)_2\cdot$MeCN	$[Cu^{II}(\mathbf{3})](ClO_4)_2$
Formula	$C_{16}H_{26}Cl_2CuN_6O_{12}$	$C_{18}H_{29}Cl_2CuN_7O_{12}$	$C_{18}H_{33}Cl_2CuN_6O_{5.5}$	$C_{34}H_{62}Cl_4Cu_2N_{11}O_{6.5}$	$C_{18}H_{31}CuN_7O_6$	$C_{18}H_{30}Cl_2CuN_6O_{10}$	$C_{16}H_{27}Cl_2CuN_5O_{10}$
M	628.88	669.93	555.96	997.82	505.04	624.93	583.88
Crystal system	monoclinic	triclinic	orthorhombic	monoclinic	triclinic	monoclinic	monoclinic
Space group	$P2_1/c$ (no. 14)	P-1 (no. 2)	$Pbca$ (no. 61)	$P2_1/n$ (no. 14)	P-1 (no. 2)	$P2_1/n$ (no. 14)	$P2_1/n$ (no. 14)
a [Å]	10.850(2)	8.034(2)	16.012(2)	15.284(1)	9.094(3)	14.623(3)	7.726(3)
b [Å]	13.510(3)	9.452(2)	8.742(2)	17.598(1)	11.082(2)	12.515(3)	18.477(10)
c [Å]	16.975(8)	18.277(3)	35.516(7)	17.430(1)	12.948(2)	14.864(3)	16.006(8)
α [°]	90	79.894(12)	90	90	93.023(25)	90	90
β [°]	94.969(12)	83.490(16)	90	99.454(1)	109.011(20)	101.631(18)	94.54(2)
γ [°]	90	79.058(17)	90	90	106.694(32)	90	90
V [Å^3]	2479.0(14)	1336.9(5)	4971.3(16)	4624.3(3)	1166.25(55)	2664.4(10)	2277.7(19)
Z	4	2	8	4	2	4	4
Unique refl.	7197	4705	4362	8203	4111	4669	3970
Strong data [$I_O>2\sigma(I_O)$]	5184	3676	3632	6533	3534	3485	3330
$R1$, $wR2$	0.0754, 0.1898	0.0761, 0.1605	0.0719/0.1474	0.0469/0.1277	0.0560/0.1281	0.0789/0.1924	0.0800/0.1939

(strong data)							
*R*1, *wR*2 (all data)	0.1083, 0.1898	0.1030, 0.1846	0.0859/0.1534	0.0684/0.1422	0.0603/0.1386	0.1062/0.2198	0.0948/0.2091

■ ASSOCIATED CONTENT

Supporting information

X-ray crystallographic files in CIF format and plots showing thermal ellipsoids for the studied molecular crystals. Details on the spectrophotometric titrations in MeCN.
This material is available free of charge via the Internet at http://pubs.acs.org.

■ AUTHOR INFORMATION

Corresponding Author:

* E-mail: luigi.fabbrizzi@unipv.it

Notes

The authors declare no competing financial interest.

■ ACKNOWLEDGEMENTS

The financial support of the Italian Ministry of University and Research (PRIN–InfoChem) is gratefully acknowledged.

■ REFERENCES

(1) Boiocchi, M.; Fabbrizzi, L.; Maurizio Licchelli, M.; Sacchi, Vázquez-López, M.; Zampa, C. *Chem. Commun.* **2003**, 1812−1813.

(2) Chae, M. Y.; Czarnik, A. W. *J. Am. Chem. Soc.* **1992**, *114*, 9704-9705.

(3) Lindoy, L. F. *The Chemistry of Macrocyclic Ligand Complexes*, Cambridge University Press, Cambridge, UK, 1989.

(4) Barefield, E. K. *Coord. Chem. Rev*. **2010**, *254*, 1607–1627.

(5) Boiocchi,M.; Fabbrizzi, L.; Foti,F.; Monzani,E.; Poggi, A. *Org. Lett.* **2005**, *7*, 3417–3420.

(6) (a) Larson. J. W.; McMahon, T. B. *Inorg. Chem.* **1984**, *23*, 2029; (b) Gronert, S. *J. Am. Chem. Soc.* **1993**, *115*, 10258-10266.

(7) Boiocchi, M.; Del Boca, L.; Gómez-Esteban, D.; Fabbrizzi, L.; Licchelli, M.; Monzani, E. *J. Am. Chem. Soc.* **2004**, *126*, 16507−16514.

(8) Boiocchi, M.; Del Boca, L.; Gómez-Esteban, D.; Fabbrizzi, L.; Licchelli, M.; Monzani, E. *Chem. Eur. J.* **2005**, *11*, 3097− 3104.

(9) Gómez-Esteban, D.; Fabbrizzi, L.; Licchelli, M.; Monzani, E. *Org. Biomol. Chem.* **2005**, *3*, 1495-1500.

(10) Gómez-Esteban, D.; Fabbrizzi, L.; Licchelli, M. *J. Org. Chem.* **2005**, *70*, 5717-5720.

(11) Amendola, V.; Fabbrizzi, L.; Gómez, D. E.; Licchelli, M. *Acc. Chem. Res.* **2006,** 39, 343-353.

(12) Farrugia, L. J. *J. Appl. Crystallogr.* **1999**, 32, 837-838.

(13) North, A. C. T.; Phillips, D. C.; Mathews, F. S. *Acta. Crystallogr.* **1968**, A24, 351-359.

(14) SAINT Software Reference Manual, Version 6, Bruker AXS Inc.: Madison, WI, USA, **2003**.

(15) Sheldrick, G. M.: SADABS Siemens Area Detector Absorption Correction Program, University of Göttingen: Göttingen, Germany, **1996**.

(16) Altomare, A.; Burla, M. C.; Camalli, M.; Cascarano, G. L.; Giacovazzo, C.; Guagliardi, A.; Moliterni, A. G. G.; Polidori, G.; Spagna, R. *J. Appl. Crystallogr.* **1999**, 32, 115-119.

(17) Sheldrick, G. M. *Acta Crystallogr.* **2008**, A64, 112-122.

For Table of Contents Only

Macrocycles containing a nitrophenyl substituent directly linked to a nitrogen atom incorporate irreversibly a copper(II) ion with substantial change of absorption spectra in the UV and visible regions, thus behaving as optical dosimeters. When in the *ortho* position of the phenyl substituent, the nitro group coordinates the Cu^{II} center according to a scorpionate mode, while the complex moves from a *trans-I* to a *trans-III* configuration. On anion coordination (e.g. chloride), the nitro group detaches.